Spin switching and unusual exchange bias in the single-crystalline $GdCrO_3$ compensated ferrimagnet

I. Fita,[1,*] R. Puzniak,[1] A. Wisniewski,[1] and V. Markovich[2]

[1]*Institute of Physics, Polish Academy of Sciences, Aleja Lotnikow 32/46, PL-02668 Warsaw, Poland*

[2]*Department of Physics, Ben-Gurion University of the Negev, P.O. Box 653, 8410500 Beer-Sheva, Israel*

(Received 16 July 2019; published 18 October 2019)

An unusual exchange bias (EB) effect in single-crystalline $GdCrO_3$ compensated ferrimagnet (fM), composed of two antiferromagnetically coupled Gd and Cr sublattices, presenting two opposite ferromagnetic (FM) moments, is reported. It is shown that the temperature- or field-induced fast reversal of the net FM moment in $GdCrO_3$ may be identified as a switching between two opposite spin configurations, attendant with abrupt drop in Zeeman energy $\approx k_B(7 \times 10^{-4}\,\mathrm{K})$ per formula unit. It was found that the FM moment reversal is exchange biased in the narrow temperature interval above the compensation temperature $T_{comp} = 144$ K. Namely, the EB field emerges and diverges upon approaching T_{comp} at temperatures $T > T_{comp}$ while unexpectedly it collapses to zero below T_{comp}. This is in contrast to experimental results obtained for compensated fMs $RFeO_3$ (R = Nd, Sm, Er) orthoferrites showing EB in a narrow range, both above and below T_{comp}. We suppose that breakdown of EB in $GdCrO_3$ may be linked to the lack of anisotropy of the spin-only Gd S-ion magnetic moment dominating below T_{comp}.

DOI: 10.1103/PhysRevB.100.144426

I. INTRODUCTION

Ferrimagnetic (fM) orthochromite $GdCrO_3$ has currently attracted enormous interest because of its possible applications, such as fast spin switching, a phenomenon of negative magnetization, ferroelectricity, magnetoelectric effect, and giant magnetocaloric effect [1–6]. The antisymmetric exchange Dzyaloshinskii-Moriya (DM) interaction between Cr^{3+} spins and antiferromagnetic (AFM) interaction between Gd^{3+} and Cr^{3+} spins are believed to be mainly responsible for these effects. Due to the DM interaction, the weak ferromagnetic (FM) moment results from the canted AFM ordering of Cr spins below $T_N \approx 170$ K, while the opposite paramagnetic moment of Gd spins appears owing to a strong AFM coupling between Gd^{3+} and Cr^{3+} ions [7,8]. For that reason, $GdCrO_3$ exhibits a specific compensation temperature T_{comp}, at which the two opposite moments cancel each other so the net magnetization vanishes, while below T_{comp} the net FM moment is aligned oppositely to the moderate applied magnetic field and hence demonstrates a negative magnetization in a broad temperature range ~100 K. Similar compensated fM spin structures have been identified in various orthorhombic perovskites RMO_3 (R = rare-earth ions; M = Fe, Cr, Mn) [9–17] and the singular configuration of spins was confirmed by the density functional theory calculations in the case of $NdFeO_3$ [11].

Remarkable interest is presently expanded to the compensated fM materials that demonstrate the exchange bias (EB) effect coexisting together with exotic spin switching and negative magnetization [13–21]. Conventional EB effect is usually associated with a shift in magnetization hysteresis loop which emerges due to the exchange interaction at the interface between hard anisotropic AFM and soft FM phases [22,23]. The origin of EB discovered in the single-phase fMs without phase interface is very different and it connects to the intrinsic exchange coupling between opposing spins inside the unit cell. This is why some bulk fMs demonstrate a gigantic EB. It was first proposed by Webb *et al.* [24] that the EB field H_{EB}, inversely proportional to the net FM moment, occurs at the T_{comp} of fM comprising two AFM coupled sublattices with opposite FM moments. This is in some resemblance to standard interfacial EB, as the EB field is inversely proportional to the saturation magnetization and thickness of ferromagnet [22,23]. Sun *et al.* [13] recently proposed a similar phenomenological model for EB in single-phase fM, in which coupling between two magnetic sublattices J_{INT} plays the same role as the interfacial exchange interaction between two separate AFM and FM phases in conventional EB. This model explains well the singular EB behavior recently found in single-crystalline $RFeO_3$ (R = Nd, Sm, Er) orthoferrites. Namely, the EB field diverges and changes sign at T_{comp} when the net FM moment approaches zero and changes its direction to the opposite one with crossing T_{comp}. The exceptional EB features of orthoferrites motivate the studies of EB in $GdCrO_3$ orthochromite exhibiting the identical fM structure while this compound has a much higher compensation temperature T_{comp}. In this paper, we show that the FM moment reversal in $GdCrO_3$ is indeed likewise exchange biased around T_{comp} but the EB behavior cardinally differs from that found for compensated orthoferrites. Namely, the EB exists only in the narrow temperature interval above $T_{comp} = 144$ K and EB sharply increases upon approaching T_{comp}, while unexpectedly it collapses to zero below T_{comp}. The unique disappearance of EB below T_{comp} is caused likely by the dominated spin-only soft magnetic moment of the Gd S ion.

*Corresponding author: ifita@ifpan.edu.pl

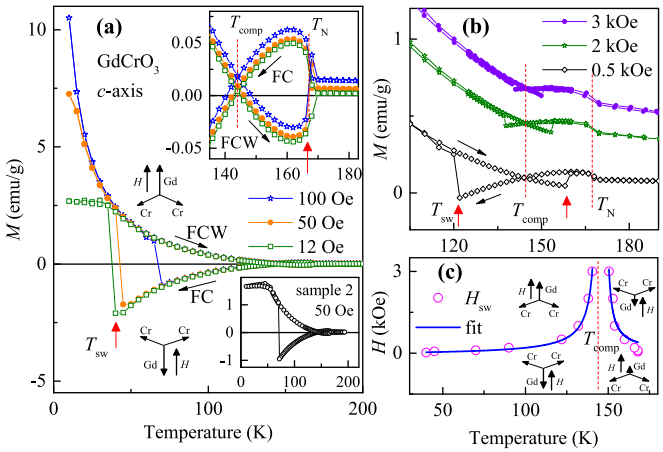

FIG. 1. (a) Temperature dependence of magnetization of $GdCrO_3$ single crystal measured along the c axis upon field cooling (FC) and subsequently on warming (FCW) at external magnetic field of 100, 50, and 12 Oe. Two possible spin configurations above and below the spin-switching (magnetization-reversal) temperature T_{sw} are shown. The upper inset shows FC and FCW magnetizations around the compensation point $T_{comp} = 144$ K. The lower inset shows the spin switching at 50 Oe of external magnetic field directed along the c axis in the sample 2 with much larger demagnetization factor $4\pi N = 4.27$. (b) Spin switching around T_{comp} at higher magnetic fields. (c) The $T_{sw} - H_{sw}$ boundary between phases with different spin configurations, with H_{sw} field values corrected for the demagnetization field. The lines represent fit with $H_{sw} \propto T/(T - T_{comp})$ dependence.

II. EXPERIMENTAL DETAILS

Magnetization measurements were performed on a $GdCrO_3$ single crystal with dimensions $3.3 \times 2 \times 0.2\,mm^3$ in the temperature range 10–200 K and in magnetic field up to 10 kOe, using a PAR (Model 4500) vibrating sample magnetometer. Temperature- and field-dependent magnetization was measured along the FM easy axis, along which the magnetization reverses sharply, changing the direction by 180°. The easy magnetic axis is the c axis of the crystal coincided with the widest face of the plate which was cut from the original crystal, oriented using x-ray diffraction. The angular dependence of magnetization was also assessed to adjust the c-axis orientation with respect to the applied magnetic field. The calculated demagnetizing factor of the sample $4\pi N = 0.78$ was used for values of magnetic field correction.

III. RESULTS AND DISCUSSION

Figure 1(a) presents the temperature dependences of magnetization of $GdCrO_3$ measured along the c axis at fields of 100, 50, and 12 Oe for field-cooling (FC) and field-cooling-warming (FCW) modes. One can recognize three successive magnetic transitions that occur at (i) the Néel temperature $T_N = 167$ K at which the noncollinear AFM order of Cr spins following a weak FM moment fixed along the c axis appears; (ii) the compensation temperature $T_{comp} = 144$ K at which two opposite magnetic moments, the FM moment of Cr spins and paramagnetic moment of Gd spins induced by the AFM coupling between Cr^{3+} and Gd^{3+} ions, annul each other so that the net magnetization vanishes; (iii) the field-dependent spin switching temperature T_{sw} at which the magnetization reverses suddenly, changing its sign from the negative to the positive one. The metastable state with negative magnetization (which means that the net magnetic moment aligns oppositely to the applied field) appears below T_{comp} when measurements are performed in the FC mode, while it develops above T_{comp} in the case of the FCW mode (see inset in Fig. 1). Two appropriate spin configurations, above and below the switching temperature T_{sw}, are shown in Figs. 1(a) and 1(c). The transition between opposite spin alignments (the change from negative magnetization to the positive one at small field H) becomes possible when the concomitant fall in Zeeman energy is large enough to reverse the spins in the crystal. In this view, the abrupt spin reversal labels the boundary of phase lability at the first-order transition. With increasing magnetic field, the gap between the switching temperatures T_{sw} occurring below and above T_{comp} (that is a hysteresis width of magnetic transition at T_{comp}) decreases from 120 K at 50 Oe to 10 K at 3 kOe [see Fig. 1(b)]. The boundaries between phases of different spin configurations, at T_{sw} vs H plane, above and below T_{comp} are presented in Fig. 1(c). It appears that the switching field, H_{sw}, increases enormously at approaching temperature T_{comp} because the opposite Cr and Gd moments become balanced and the difference between diverse spin alignments vanishes.

It was shown by Cooke *et al.* [7] that the peculiar fM behavior of $GdCrO_3$ may be reasonably well explained within the simple model taking into account the canted FM moment of Cr spins, due to the DM interaction, and the opposite paramagnetic moment of Gd^{3+} induced by the AFM interaction between Cr^{3+} and Gd^{3+} spins. In this model, the temperature dependence of magnetization can be expressed as

$$M = M_{Cr} + C_{Gd}(-H_I + H)/(T + \theta), \qquad (1)$$

where M_{Cr} is the canted magnetization of the Cr sublattice; C_{Gd} is the Curie constant; $C = Ng^2\mu_B{}^2 S(S+1)/3k_B$, equal to 0.0306 emu K/g according to calculation for the Gd^{3+} ground state with spin $S = 7/2$; H_I is the internal exchange field generated by the ordered Gd sublattice in opposed direction to the magnetization M_{Cr}; H is the applied field; and θ is the Weiss constant linked to the interaction between Gd^{3+} spins. Equation (1) has been frequently used for successful fitting of the field and temperature dependences of magnetization in $GdCrO_3$ [3,7,8]. Here, we show that this phenomenological model qualitatively describes also the sudden spin switching that occurs around the T_{comp} in $GdCrO_3$. We assume that the spontaneous spin switching is caused by a momentary fall in Zeeman energy $E_Z = -MH$ required for the concomitant spin structure transformation. For simplicity, we ignore here the insubstantial interaction between Gd^{3+} spins ($\theta = 2.3$ K has been determined in Ref. [7]) fixing in Eq. (1) the $\theta = 0$. According to Eq. (1), the E_Z is maximal for the spin configuration realizing metastable state with negative magnetization: $E_{Z1} = -[M_{Cr} + C_{Gd}(-H_I + H)/T]H$, and is minimal for the state with magnetization parallel to the applied field H: $E_{Z2} = -[-M_{Cr} + C_{Gd}(H_I + H)/T]H$. Thus, the change in Zeeman energy $\Delta E = E_{Z1} - E_{Z2}$ at the spin

switching is equal to $\Delta E = -2(M_{Cr} - C_{Gd}H_I/T)H_{sw}$. Then, taking into account that $T_{comp} = C_{Gd}H_I/M_{Cr}$, determined according to Eq. (1) as the temperature at which $M = 0$ at $H = 0$, the switching field H_{sw}, as a function of temperature, can be expressed as follows:

$$H_{sw} = \pm(\Delta E/2M_{Cr})T/(T - T_{comp}), \qquad (2)$$

where "+" is an appropriate sign for the temperature region $T > T_{comp}$ and "−" is the actual sign for the $T < T_{comp}$ one. The obtained H_{sw} vs T dependence, with switching field $H_{sw} = H - 4\pi NMd$ corrected for the demagnetization factor, was verified with experimental data assuming that the $\Delta E/M_{Cr}$ ratio is constant. The solid lines in Fig. 1(c) are the best fit with Eq. (2) for the values of fitting parameters $\Delta E/2M_{Cr} = 103 \pm 4$ Oe and $T_{comp} = 145.3 \pm 0.2$ K, calculated for the region $T < T_{comp}$. A poorer fit is obtained for the $T > T_{comp}$ region, possibly because the M_{Cr} value somewhat changes at approaching the Néel temperature. Using the value of canted moment $M_{Cr} = 1.15$ emu/g, determined here by analysis of M vs T dependence (see text below), we calculate the energy $\Delta E = 237$ erg/g $\approx k_B(7 \times 10^{-4}$ K) per formula unit. It appears that the identical change in Zeeman energy ΔE occurs at spin reversal on the $T_{sw} - H_{sw}$ boundary shown in Fig. 1(c). Therefore, the parameter ΔE is a characteristic for $GdCrO_3$.

The magnetization curve at the smallest measured field of 12 Oe [see Fig. 1(a)] shows the transition at 35 K from the single-domain magnetization state to the multidomain structure below which M remains constant. It occurs because below 35 K the demagnetizing field $4\pi NMd$ compensates the external field, so the effective field inside the sample becomes equal to zero and the volume magnetic susceptibility $\chi_v = Md/H$ keeps a constant value of $1/4\pi N$. Here, M is the mass magnetization and $d = 7.3$ g/cm^3 is the density of the $GdCrO_3$ crystal. Indeed, one can see that below 35 K the susceptibility $\chi_v = (2.5$ emu/g$) \times (7.3$ g/cm$^3)/12$ Oe $\approx$ 1.5 is close to the value $1/(4\pi N) \approx 1.3$, where the calculated demagnetizing factor of sample $4\pi N = 0.78$. In order to prove the nature of magnetic transition at 35 K, we have investigated the spin switching at $H = 50$ Oe in another $GdCrO_3$ crystalline sample, described as sample 2, with dimensions $2.6 \times 1.7 \times 1.3$ mm^3 and a much larger demagnetizing factor $4\pi N = 4.27$ for the H direction along the 1.7 mm face (c axis) [see FC and FCW magnetizations presented in the lower inset of Fig. 1(a)]. For this sample, the susceptibility χ_v achieves a constant value close to $1/4\pi N$ below 53 K, signifying the transition to the multidomain magnetic state. This happens since the enlarged demagnetizing field of sample 2 compensates the applied field of 50 Oe already at 53 K : $4\pi NMd = 4.27 \times (1.6$ emu/g$) \times (7.3$ g/cm$^3) \approx 50$ Oe. Similarly, the spin reversal occurs at a much higher temperature of 71 K as compared to that in the sample with smaller demagnetization factor N. Correcting the magnetic field inside the sample at the beginning of spin reversal, we get the real switching field $H_{sw} = H - 4\pi NMd = 50$ Oe $- 4.27 \times (-0.96$ emu/g$) \times (7.3$ g/cm$^3) \approx 80$ Oe at 71 K which agrees well with the $T_{sw} - H_{sw}$ boundary shown in Fig. 1(c). It should be noted that the spin reversal at 50 Oe field has been observed previously in the $GdCrO_3$ crystal at 75 K [3]. The authors of Ref. [3] did not report the value of the factor N for their sample but they noted that the crystals were of millimeter size. In such case, a value of $4\pi N$ between 4 and 5 may be expected, being in good agreement with our data. The above comparison shows that the accurate estimation of the value of demagnetizing factor N is important for determination of the true spin switching parameters at low fields and temperatures.

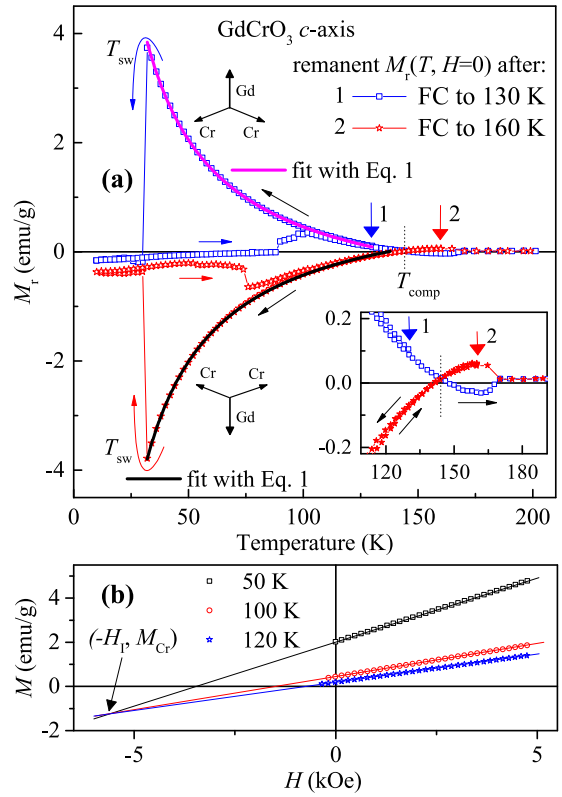

FIG. 2. (a) Remanent magnetization M_r, measured along the c axis upon cooling at $H = 0$, after FC with $H = 10$ kOe to temperature (1) $T = 130$ K $< T_{comp}$ and (2) $T = 160$ K $> T_{comp}$. The M_r obtained with different cooling protocol shows the alternating sign. A sharp fall in M_r at $T_{sw} = 32$ K indicates a transition from the single-domain state to the multidomain one with $M \approx 0$. The lines are the best fit with Eq. (1). (b) M vs H curves along the c axis at several temperatures. The extrapolated lines intersect, in accordance with Eq. (1), at $H = -H_I = -5.6$ kOe and $M = M_{Cr} = -1.22$ emu/g.

In order to understand better the origin of spin reversal in $GdCrO_3$, we examined the temperature dependences of remanent magnetization M_r along the c axis, recorded at $H = 0$ upon cooling and subsequently on warming, after FC with $H = 10$ kOe from room temperature; see Fig. 2(a). Two different FC regimes were employed. In the first one, the FC was extended to a temperature below T_{comp}, $T = 130$ K, making the M_r positive at the starting temperature because the dominant here Gd paramagnetic moment has been aligned with the cooling field. With subsequent lowering of T at $H = 0$, the M_r increases on account of Curie-Weiss (CW) -like increase of the Gd moment governed by the internal field H_I from the ordered Cr spins. In the second regime, the FC was finished at temperature $T = 160$ K $> T_{comp}$; therefore the opposite spin configuration with FM moment M_{Cr} along the cooling field has been fixed [see spin schematics in Fig. 2(a)],

and then at $T < T_{comp}$ the M_r is opposite to the one appearing at the cooling with the first mode. One can see in Fig. 2(a) that M_r measured with different modes is almost identical in value but has the opposite sign depending on the FC procedure. Interestingly, a sharp fall in M_r to almost zero value (magnetization switching occurs in the absence of external magnetic field) is observed at both $M_r(T)$ branches at the same temperature of 32 K. At this temperature, the $|M_r|$ reaches a value of 3.8 emu/g = 28 emu/cm^3, so the corresponding demagnetizing field $H_d = -4\pi NMd \approx 22$ Oe becomes large enough to cause the reversal of the previous spin configuration in a fraction of the sample volume, leading to a multidomain state with $M \approx 0$. Indeed, one can see that the change in Zeeman energy at the transition $MH_d \approx 84$ erg/g is about three times less than the energy ΔE required for the magnetization reversal in the total volume of the sample. Based on these facts, the sharp drop in remanent magnetization at 32 K may be identified as a transition from the single-domain state with uniform magnetization to the multidomain one with $M \approx 0$.

Intriguingly, during the reverse warming process at $H = 0$, the former single-domain state is restored at much higher temperatures, ~100 K [see Fig. 2(a) and the inset therein], and the reinstalled magnetization preserves its previous direction; i.e., the magnetic system remembers its previous spin configuration which has been fixed by the cooling field at high temperatures. Notice also that the large temperature hysteresis conceived is indicative of the first-order nature of the transition.

Both $M_r(T)$ branches of remanent magnetization, obtained with different modes 1 and 2, were examined within the model which assumes Eq. (1) with approximation of noninteracting Gd^{3+} spins. The solid lines in Fig. 2(a) are the best fit with Eq. (1), where $\theta = 0$, $H = 0$, and $C_{Gd} = 0.0306$ emu K/g Oe are fixed, for the following values of fitting parameters: $M_{Cr} = -1.136 \pm 0.006$ emu/g and $H_I = +5.2 \pm 0.015$ kOe (for mode 1), and $M_{Cr} = +1.158 \pm 0.003$ emu/g and $H_I = -5.18 \pm 0.01$ kOe (for mode 2). The signs of M_{Cr} and H_I indicate that the canted moment M_{Cr} and field H_I are opposite to each other and their directions are also changed to the opposite ones when the FC procedure changes. The almost identical values of M_{Cr} and H_I are obtained for the different measurement modes, and they are close to the values $M_{Cr} = 1.55$ emu/g and $H_I = 5.5$ kOe, formerly found by Cooke *et al.* [7] by analysis of the field dependences of magnetization. Additionally, we repeated the same analysis, illustrated in Fig. 2(b), where the M vs H curves along the c axis at several temperatures are presented. The extrapolated lines intersect, in accordance with Eq. (1), at a common point with $H = -H_I = -5.6$ kOe and $M = M_{Cr} = -1.22$ emu/g. The obtained M_{Cr} and H_I values are in good agreement with those determined at $H = 0$, based on the remanent magnetization data, and the calculated temperature $T_{comp} = C_{Gd}H_I/M_{Cr} \approx 140$ K is close to the experimental one. It follows also from the Cooke *et al.* analysis, successfully exploited for the $GdCrO_3$ crystal also in Ref. [3], that the linear increase of magnetization with magnetic field shown in Fig. 2(b) is mainly due to the paramagnetic noninteracting spins of Gd^{3+} contribution and the slope of the M vs H curves is equal to the C_{Gd}/T, in accordance with Eq. (1).

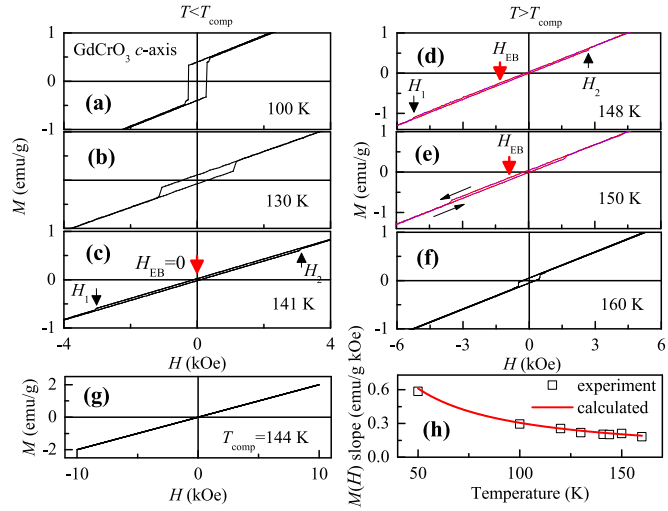

FIG. 3. Magnetization hysteresis loops of $GdCrO_3$, in an extended scale, measured between ±10 kOe and with cooling field 10 kOe along the c axis at temperatures $T < T_{comp} = 144$ K (a)–(c) and at $T > T_{comp}$ (d)–(f). Arrows indicate the fields of the first and the second magnetization reversals, H_1 and H_2, respectively, and EB field H_{EB}. The ascending and descending loop branches around H_1 are also indicated (e). (g) The magnetization loop at T_{comp}. (h) The calculated C_{Gd}/T and measured $M(H)$ slopes in the temperature range between 50 and 160 K.

Further, we study the field-induced spin switching which has the same origin as the spontaneous spin transition accomplished at constant magnetic field. Figure 3 presents the magnetization hysteresis loops of $GdCrO_3$ measured along the c axis at several temperatures above and below T_{comp} between ±10 kOe and with a cooling field of 10 kOe. The $M(H)$ loop of compensated fM may be considered practically as a sum of two separate contributions, interpreted within the phenomenological model according to Eq. (1), comprising the opposite alignment of paramagnetic moment Gd spins with respect to the FM moment of canted Cr spins M_{Cr} and with assumption that $\theta = 0$ and M_{Cr} is unchanged. The first contribution is the linear field-dependent paramagnetic magnetization $C_{Gd}H/T$ originated from the Gd spins, where C_{Gd}/T is the $M(H)$ slope. The shape of hysteresis loop at the T_{comp} is identical with the straight line, with the slope calculated with the above fit parameters, $C_{Gd}/T_{comp} = M_{Cr}/H_I = 0.21$ emu/(g kOe); see Fig. 3(g). Figure 3(h) shows that both calculated and measured $M(H)$ slopes practically coincide in the temperature range between 50 and 160 K. The second component of the loop is the compensated net FM moment, equal to the residual $M_{Cr} - C_{Gd}H_I/T$ in accordance with Eq. (1). With varying magnetic field, the FM moment sharply reverses at switching fields H_1 and H_2, that are in fact the coercive fields at the first and second magnetization reversals, respectively, at which the magnetization changes by the quantity $2(M_{Cr} - C_{Gd}H_I/T)$ according to the above model. The net FM moment becomes small as temperature approaches T_{comp} and the loop becomes flattened, while the H_1 and H_2 coercive fields increase enormously because the energy change $\Delta E = -2(M_{Cr} - C_{Gd}H_I/T)H_{sw}$ at spin switching must be constant. Far from the T_{comp}, the loop becomes narrow and the

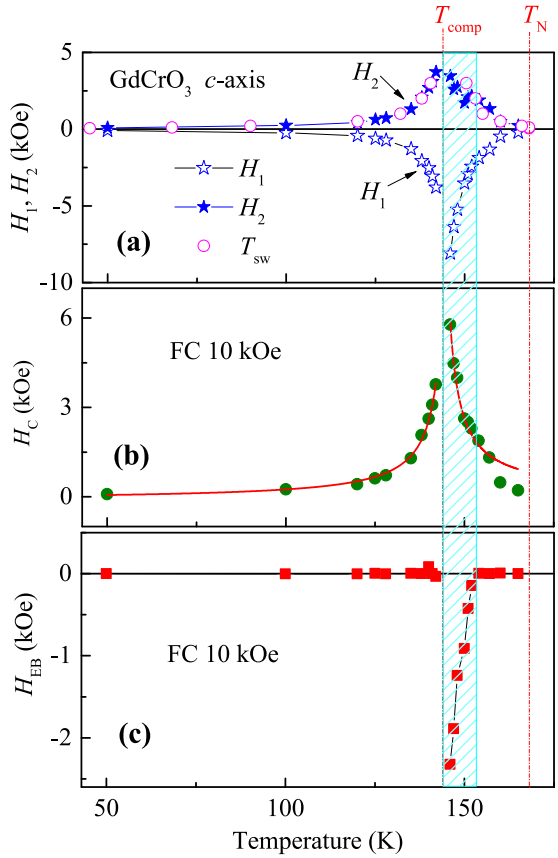

FIG. 4. Temperature variation of (a) coercive fields H_1 and H_2 at the first and second magnetization reversals, respectively [the H_{sw} vs T dependence shown in Fig. 1(c) is also presented for comparison], (b) average coercive field H_C [the lines are fit with $H_C \propto T/(T - T_{comp})$ law], and (c) exchange bias field H_{EB} for $GdCrO_3$ with applied magnetic field along the c axis. Exchange bias exists in the narrow temperature interval (marked by shadow area) above T_{comp}, and EB collapses to zero at $T < T_{comp}$.

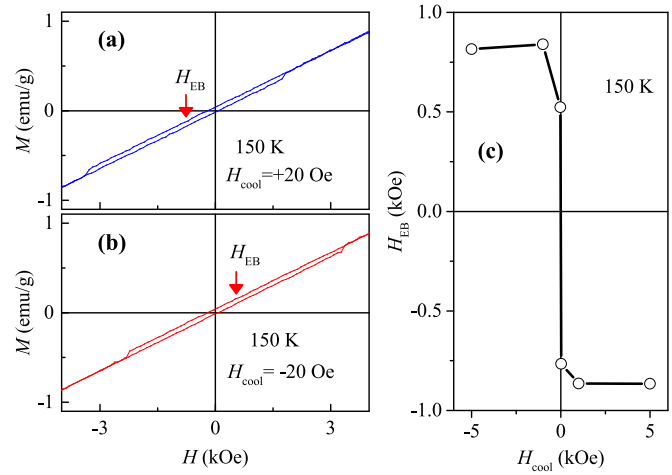

FIG. 5. Magnetization loops of $GdCrO_3$ measured between ±10 kOe at 150 K with two opposing small cooling fields $H_{cool} = +20$ Oe (a) and −20 Oe (b). The field H_{EB} changes sign with altering the H_{cool} sign. (c) The H_{EB} vs H_{cool} dependence at 150 K.

magnetization jump is large. It was found that in the whole interval below T_{comp} the $M(H)$ loops are fairly symmetric indicating the absence of exchange bias effect, i.e., the EB field defined as $H_{EB} = (H_1 + H_2)/2$ is equal to zero. In distinct contrast, at temperatures above T_{comp} and very close to T_{comp}, the center of the loop shifts from the origin to the left side, revealing the negative EB effect, $H_{EB} < 0$ [see Figs. 3(d) and 3(e)].

The coercive fields H_1 and H_2 determined from the $M(H)$ loops at various temperatures are presented in Fig. 4(a). The H_{sw} vs T dependence obtained above, based on the $M(T, H = \text{const.})$ curves [see Fig. 1(c)], is also presented here for comparison. It is seen that the positive coercive field H_2 coincides well with the spontaneous switching field H_{sw}, clarifying that the switching between two contrary spin configurations, shown in Fig. 1(c), occurs in fact at the fields H_1 and H_2. Consequently, the FM moment reversal in the course of the $M(H)$ loop may be considered as the first-order transition spreading in a field with the hysteresis width of quantity $H_2 - H_1$, which increases significantly upon approaching temperature T_{comp}, where the difference between the two spin configurations disappears. The average coercive field $H_C = (H_2 - H_1)/2$ is shown in Fig. 4(b), where solid lines are the best fit with Eq. (2). The values of fitting parameters $\Delta E/2M_{Cr} = 114 \pm 6$ Oe and $T_{comp} = 146.2 \pm 0.3$ K obtained for temperatures below T_{comp} are in good agreement with those calculated above based on the spontaneous spin switching data. The poorer quality of the fit gotten for the interval $T > T_{comp}$ is caused most likely by impact of the existing EB in the vicinity of T_{comp} and/or by the M_{Cr} changes when temperature approaches the T_N.

Figure 4(c) presents the temperature dependence of exchange bias field H_{EB} obtained after the FC with 10 kOe applied along the c axis. With lowering temperature, the EB field emerges and increases rapidly in the narrow interval of a few kelvin upon approaching T_{comp}, while unexpectedly it collapses to zero when the temperature crosses T_{comp}, and H_{EB} remains zero in the whole interval $T < T_{comp}$. Thus, the EB exists in $GdCrO_3$ above T_{comp} only, in the temperature interval of a width of ∼8 K in which the H_1 and H_2 fields differ in value and the coercive field H_C is enlarged [see Figs. 4(a) and 4(b)]. The cooling field effect on EB shown in Fig. 5 may illuminate the nature of the EB. Figures 5(a) and 5(b) demonstrate two magnetization loops recorded at 150 K with the same field variation protocol (from +10 to −10 kOe, and then to +10 kOe) but with small cooling fields of different signs, $H_{cool} = +20$ Oe and −20 Oe. It appears that the change of sign of such small cooling field is capable of changing the sign of the EB. This means that the fM system memorizes exactly the spin configuration, which has been established by small field H_{cool} during the FC process, despite the strong field of 10 kOe having been applied next at 150 K. Physically, the EB sign is determined by the initial direction of the net FM moment; namely, is it parallel or against to the applied magnetic field. Thus, the obtained EB depends on whether the H_{cool} was applied with positive or negative polarity; i.e. there is a memory effect and the EB is easy switchable. The sign of field H_{cool} determines the EB sign, and EB saturates at cooling fields higher than 1 kOe; see symmetrical H_{EB} vs H_{cool} dependence at 150 K in Fig. 5(c).

The exotic EB in $GdCrO_3$ differs remarkably from that recently observed in compensated fMs $RFeO_3$ (R = Nd, Sm, Er) orthoferrites that show EB in a narrow range both above and below T_{comp}. Additionally the EB was found to diverge approaching T_{comp} from both sides, and EB changes its sign when the temperature crosses T_{comp} [16]. Furthermore, the very analogous change of the EB sign at T_{comp} has been detected also in several other compensated fM systems [18–21,24], so the puzzling disappearance of EB below T_{comp} in $GdCrO_3$ is a unique feature among them. We discuss this intriguing issue using the model proposed by Sun *et al*. [13] for EB in a single-phase fM where the coupling between two magnetic sublattices J_{INT} induces the EB in the same manner as it is generated by the interfacial exchange interaction between two separate AFM and FM phases in the conventional EB systems. In this model, within approximation of very strong anisotropy of an AFM ordered sublattice, the field H_{EB} is determined by the ratio of the coupling constant J_{INT}, that is, the AFM interaction between $4f$ and $3d$ ions, to the net (compensated) FM moment M_{net} [17]:

$$H_{EB} = J_{INT}/M_{net}\cos\phi, \tag{3}$$

where ϕ is the angle between M_{net} and field H. The expression (3), which is reminiscent of the well-known formula of the Meiklejohn-Bean (MB) model of conventional FM/AFM interface EB [22,23], is obtained within the same strong restrictions as that in the MB model. As discussed in Refs. [13,17], the EB exists only when the anisotropy energy of ordered AFM sublattice is large enough and it predominates over J_{INT} energy [13]. In the case of a large AFM anisotropy, similar to that occurring at a FM/AFM interface in the case of conventional EB, the spin rotation of the FM sublattice experiences the pinning force from the hard AFM sublattice; therefore EB could be expected [13]. On the contrary, if there is a strong coupling between two sublattices J_{INT} prevailing over the AFM anisotropy energy, both the AFM and FM spins should rotate together and no EB appears. This model is capable to explain qualitatively the peculiar EB features of $GdCrO_3$ presented in Figs. 4(c) and 5. As the temperature approaches T_{comp}, the EB appears when the spontaneous net FM moment M_{net}, which is equal to $M_{Cr} - C_{Gd}H_I/T$ in accordance with Eq. (1), becomes small enough to be pinned by the hard AFM sublattice, and with further lowering of the temperature M_{net} diminishes rapidly. Therefore, the EB increases strongly in accordance with Eq. (3). In the case of positive H_{cool}, which requires that both M_{net} and applied field H are parallel, so that $\phi = 0$ or $\cos\phi = 1$, the EB is negative according to Eq. (3) where $J_{INT} < 0$. Conversely, the negative H_{cool} fixes antiparallel M_{net} and field H; hence $\phi = \pi$, then $\cos\phi = -1$, and the EB is positive. Thus, the above model well explains the switchable EB governed by the polarity of field H_{cool} shown in Fig. 5.

Moreover, the model assuming relation (3) is compatible also with universal EB behavior of compensated $RFeO_3$ (R = Er, Nd, Sm) ferrimagnets [15,16] demonstrating the increase and divergence of EB upon approaching T_{comp} from both sides, and the change of the EB sign across T_{comp}. In these fMs, when the positive field H_{cool} is applied, the EB is positive at $T < T_{comp}$ because the moment M_{net} orients oppositely to the applied field H; hence $\phi = \pi$, $\cos\phi = -1$, and according to Eq. (3), $H_{EB} > 0$. In distinct contrast, the $GdCrO_3$ demonstrates $H_{EB} = 0$ at $T < T_{comp}$; see Fig. 4(c). We assume that this breakdown of EB upon crossing T_{comp} may occur in $GdCrO_3$ because of sudden weakening of the magnetocrystalline anisotropy of the system. Indeed, at $T < T_{comp}$ the net FM moment $M_{net} = M_{Cr} - C_{Gd}H_I/T$ is Gd spin dominant since the AFM ordered Cr spin contribution appears to be compensated. The resultant effective magnetic anisotropy of the system becomes, in general, quite small as the Gd^{3+} is an S ion ($J = S = 7/2$, $L = 0$) and the crystal field effects are expected to be absent. At such condition, the interaction energy J_{INT} dominates the tiny anisotropy of the system presented mainly by the spin-only soft magnetic moment of Gd; therefore no EB appears in a view of the above model.

It should be noted that due to the unique Gd^{3+} spin configuration among the rare-earth elements, $GdFeO_3$ orthoferrite demonstrates also the peculiar magnetic behavior, for instance, an almost isotropic and large magnetization, which is very different from that reported for other orthoferrites [25]. An important difference between $GdFeO_3$ and other orthoferrites is the lack of spin-reorientation transition in $GdFeO_3$, suggesting very weak anisotropic interaction between Gd^{3+} and Fe^{3+} moments. Probably for similar reasons, the lack of EB below T_{comp} in $GdCrO_3$ is unique among the known exchange-biased compensated fMs studied. In $RFeO_3$ (R = Er, Nd, Sm), the EB exists at $T < T_{comp}$ due to the highly anisotropic Er, Nd, and Sm magnetic moments with the significant orbital component (for both Er^{3+} and Nd^{3+} $L = 6$, according to the Hund's rules). We emphasize also another important difference: the average coercive field H_C of $GdCrO_3$ falls by ~2 kOe upon crossing T_{comp} to the region dominated by Gd^{3+} low-anisotropic moments [see Fig. 4(b)], while on the contrary the H_C of both $ErFeO_3$ and $NdFeO_3$ increases sharply with crossing T_{comp} to the region dominated by highly anisotropic moments of Er^{3+} and Nd^{3+}; see Fig. 4(b) in Ref. [16]. The different change in H_C may indicate different changes in magnetocrystalline anisotropy of the systems and the essential role of the spin-orbital interactions in the EB effect. In order to prove the above scenario experimentally, we plan hereafter to investigate the crystalline $CeCrO_3$ orthochromite with $T_N = 260$ K, $T_{comp} \approx 120$ K, and the Ce^{3+} magnetic ions with orbital momentum $L = 3$ [26].

IV. CONCLUSIONS

The temperature- and field-induced fast reversals of the net FM moment along the c axis were studied carefully in a single-crystalline $GdCrO_3$ compensated ferrimagnet. The reversal of the FM moment is associated with an abrupt switching between two opposing spin configurations which accomplishes as the first-order magnetic transition with concomitant loss in energy $\approx k_B(7 \times 10^{-4}\,\mathrm{K})$ per formula unit, and the switching field H_{sw} varies with temperature according to the $T/(T - T_{comp})$ law. It was found that the FM moment reversal is exchange biased only in a narrow temperature interval above the compensation temperature $T_{comp} = 144$ K. Specifically, the EB field emerges and diverges upon approaching T_{comp} at temperatures $T > T_{comp}$ while unexpectedly it collapses to zero below T_{comp}. This behavior cardinally

differs from that observed for compensated Er, Nd, and Sm orthoferrites which show EB at both sides in the vicinity of the T_{comp}. The puzzling loss of EB at $T < T_{comp}$ is likely associated with the lack of anisotropy of a spin-only Gd *S*-ion magnetic moment which dominates in $GdCrO_3$ below T_{comp}. Comparison of the EB effect in $GdCrO_3$ and in $RFeO_3$ (R = Er, Nd, Sm), where the EB exists at $T < T_{comp}$ due to the highly anisotropic Er, Nd, and Sm magnetic moments having the significant orbital component, indicates the essential role of the spin-orbital interactions in the EB effect.

[1] B. Rajeswaran, D. I. Khomskii, A. K. Zvezdin, C. N. R. Rao, and A. Sundaresan, Phys. Rev. B **86**, 214409 (2012).

[2] A. Kumar and S. M. Yusuf, Phys. Rep. **556**, 1 (2015).

[3] L. H. Yin, J. Yang, X. C. Kan, W. H. Song, J. M. Dai, and Y. P. Sun, J. Appl. Phys. **117**, 133901 (2015).

[4] S. Mahana, B. Rakshit, R. Basu, S. Dhara, B. Joseph, U. Manju, S. D. Mahanti, and D. Topwal, Phys. Rev. B **96**, 104106 (2017).

[5] S. Mahana, U. Manju, P. Nandi, E. Welter, K. R. Priolkar, and D. Topwal, Phys. Rev. B **97**, 224107 (2018).

[6] M. Tripathi, T. Chatterji, H. E. Fischer, R. Raghunathan, S. Majumder, R. J. Choudhary, and D. M. Phase, Phys. Rev. B **99**, 014422 (2019).

[7] A. H. Cooke, D. M. Martin, and M. R. Wells, J. Phys. C: Solid State Phys. **7**, 3133 (1974).

[8] K. Yoshii, J. Solid State Chem. **159**, 204 (2001).

[9] J.-H. Lee, Y. K. Jeong, J. H. Park, M.-A. Oak, H. M. Jang, J. Y. Son, and J. F. Scott, Phys. Rev. Lett. **107**, 117201 (2011).

[10] J.-S. Jung, A. Iyama, H. Nakamura, M. Mizumaki, N. Kawamura, Y. Wakabayashi, and T. Kimura, Phys. Rev. B **82**, 212403 (2010).

[11] S. J. Yuan, W. Ren, F. Hong, Y. B. Wang, J. C. Zhang, L. Bellaiche, S. X. Cao, and G. Cao, Phys. Rev. B **87**, 184405 (2013).

[12] S. Cao, H. Zhao, B. Kang, J. Zhang, and W. Ren, Sci. Rep. **4**, 5960 (2014).

[13] Y. Sun, J.-Z. Cong, Y.-S. Chai, L.-Q. Yan, Y.-L. Zhao, S.-G. Wang, W. Ning, and Y.-H. Zhang, Appl. Phys. Lett. **102**, 172406 (2013).

[14] Y. Cao, S. Cao, W. Ren, Z. Feng, S. Yuan, B. Kang, B. Lu, and J. Zhang, Appl. Phys. Lett. **104**, 232405 (2014).

[15] I. Fita, A. Wisniewski, R. Puzniak, V. Markovich, and G. Gorodetsky, Phys. Rev. B **93**, 184432 (2016).

[16] I. Fita, A. Wisniewski, R. Puzniak, E. E. Zubov, V. Markovich, and G. Gorodetsky, Phys. Rev. B **98**, 094421 (2018).

[17] L. Wang, L. L. Zhang, X. Zhang, M. L. Zhong, Z. C. Zhong, and G. H. Rao, Ceram. Int. **45**, 6143 (2019).

[18] I. Fita, V. Markovich, A. S. Moskvin, A. Wisniewski, R. Puzniak, P. Iwanowski, C. Martin, A. Maignan, R. E. Carbonio, M. U. Gutowska, A. Szewczyk, and G. Gorodetsky, Phys. Rev. B **97**, 104416 (2018).

[19] P. D. Kulkarni, A. Thamizhavel, V. C. Rakhecha, A. K. Nigam, P. L. Paulose, S. Ramakrishnan, and A. K. Grover, Europhys. Lett. **86**, 47003 (2009).

[20] K. Yoshii, Appl. Phys. Lett. **99**, 142501 (2011).

[21] X. Wang, S. Gao, X. Yan, Q. Li, J. Zhang, Y. Long, K. Ruan, and X. Li, Phys. Chem. Chem. Phys. **20**, 3687 (2018).

[22] W. H. Meiklejohn and C. P. Bean, Phys. Rev. **102**, 1413 (1956).

[23] J. Nogués, J. Sort, V. Langlais, V. Skumryev, S. Suriñach, J. S. Muñoz, and M. D. Baró, Phys. Rep. **422**, 65 (2005).

[24] D. J. Webb, A. F. Marshall, A. M. Toxen, T. H. Geballe, and R. M. White, IEEE Trans. Magn. **24**, 2013 (1988).

[25] M. Das, S. Roy, and P. Mandal, Phys. Rev. B **96**, 174405 (2017).

[26] M. Taheri, F. S. Razavi, Z. Yamani, R. Flacau, C. Ritter, S. Bette, and R. K. Kremer, Phys. Rev. B **99**, 054411 (2019).